Accurate study of FosPeg® distribution in a mouse model using fluorescence imaging technique and fluorescence white monte carlo simulations

Xie, Haiyan; Liu, Haichun; Svenmarker, Pontus; Axelsson, Johan; Gräfe, Susanna; Lundeman, Jesper Holm; Cheng, Haynes Pak Hay; Kyriazi, Maria; Bendsoe, Niels; Andersen, Peter E.; Svanberg, Katarina; Andersson-Engels, Stefan

Published in:
Optical Society of America. Journal B: Optical Physics

Publication date:
2010

Document Version
Publisher's PDF, also known as Version of record

Accurate Study of FosPeg® Distribution in a Mouse Model Using Fluorescence Imaging Technique and Fluorescence White Monte Carlo Simulations

Haiyan Xie[1,*], Haichun Liu[1], Pontus Svenmarker[1], Johan Axelsson[1], Susanna Gräfe[2], Jesper Holm Lundeman[3], Haynes Cheng[3], Maria Kyriazi[4], Niels Bendsoe[5], Peter Andersen[3], Katarina Svanberg[6], and Stefan Andersson-Engels[1]

1 Department of Physics, Lund University, P.O. Box 118, SE-221 00, Lund, Sweden
2 Biolitec AG, Research and Development, D-077 45, Jena, Germany
3 DTU Fotonik, DK-4000, Roskilde, Denmark
4 Biomedical Optics and Applied Biophysics Laboratory, Department of Electrical Engineering and Computing, National Technical University of Athens, G-157 80, Athens, Greece
5 Department of Dermatology and Venereology, Lund University Hospital, SE-221 85, Lund, Sweden
6 Department of Oncology, Lund University Hospital, SE-221 85, Lund, Sweden

** haiyan.xie@fysik.lth.se*

Abstract: Fluorescence imaging is used for quantitative in vivo assessment of drug concentration. Light attenuation in tissue is compensated for through Monte-Carlo simulations. The intrinsic fluorescence intensity, directly proportional to the drug concentration, could be obtained.

OCIS codes: (170.3880) Medical and biological imaging; (110.0113) Imaging through turbid media

1. Introduction

FosPeg® (biolitec AG, Jena, Germany) is a new photosensitizer based on FOSCAN, aiming to optimize its distribution properties. It is important to study the pharmacokinetics and distribution of this novel drug to better understand its potential for photodynamic therapy. Fluorescence imaging is a non-invasive and sensitive modality to follow the drug concentration. However the raw fluorescence signals from tissue surfaces recorded in the images are heavily attenuated by tissue with different optical properties. There exists a need to compensate for such attenuation. Themelis et al. developed a fluorescence imaging system using light-absorption correction based on a ratio approach of fluorescence over light attenuation images in the NIR excitation and emission [1]. We present a novel method utilizing time-resolved fluorescence white Monte Carlo (FWMC) simulations in combination with Beer-Lambert law to obtain the intrinsic fluorescence intensity originating from the fluorophores. The results from calibration on tissue phantoms have shown very good correlations between the intrinsic fluorescence intensities and dye concentrations regardless of the phantom optical properties. Our approach also offers advantages of a wide wavelength region and a very low concentration detection limit. Results from pharmacokinetic studies of FosPeg in animals are presented.

2. Materials and methods

2.1 Animal procedure and phantom preparation

The biodistribution and pharmacokinetics of FosPeg were investigated in 30 female NMRI nu/nu mice. At different intervals (30 min, 2h, 4h, 8h and 18h) after the photosensitizer injection the animals were sacrificed, and eight organs were excised (tumor, muscle, skin, liver, spleen, kidney, lung and heart) for measurements. The results from high performance liquid chromatography (HPLC) of excised tissue are used as a gold standard to be correlated to the fluorescence measurements.

A set of liquid tissue phantoms were prepared with water, intralipid, ink, and Rhodamine 6G. The relevant optical properties are chosen to be typical for tissue.

2.2 Measurements

Excitation light at 405 nm is delivered through an optical fiber mounted above the target. Images of the fluorescence, after being spectrally filtered using a liquid crystal tunable filter centered at 652 nm (corresponding to the peak emission of m-THPC), were acquired using a CCD camera. As to the phantoms, the excitation and emission are at 532 nm and 600 nm, respectively. The optical properties of the phantoms were measured with a time-of-flight spectroscopy system employing a supercontinuum white-light source [2].

2.3 Evaluation criteria

The principle of White Monte Carlo is explained in Ref. [2]. Swartling et al. showed an accelerated approach used in time-resolved fluorescence emission spectra modeling with higher computing efficiency than traditional MC [3]. Thus the FWMC simulation was used to obtain the intrinsic fluorescence inside tissue. The geometry used for the simulation is similar as shown in Ref. [3]. Furthermore, define t_1 and t_2 as the time taken from the light source to the intrinsic fluorophores by the excitation photons and from the fluorophores to the tissue surface by the emission photons, respectively. First, the fluorescence intensities $F(\mu_s^x, \mu_s^m, \mu_a^x = 0, \mu_a^m = 0, r, t_1, t_2)$ for a non-absorbing white medium with certain scattering coefficients μ_s^x and μ_s^m can be simulated through a FWMC procedure by making $\mu_a^x = 0$ and $\mu_a^m = 0$.

$$F(\mu_s^x, \mu_s^m, \mu_a^x = 0, \mu_a^m = 0, r, t_1, t_2) = \phi_{eff} \int_0^\infty \mathrm{d}z \int_0^\infty \mathrm{d}r' \int_0^{2\pi} \mathrm{d}\varphi' A(\mu_s^x, \mu_a^x = 0, r', z, t_1) E(\mu_s^m, \mu_a^m = 0, d, z, t_2) \qquad (1)$$

where $A(\mu_s^x, \mu_a^x, r', z, t_1)$ and $E(\mu_s^m, \mu_a^m, d, z, t_2)$ are the absorption probability of the excitation light and emission probability, respectively. $d = (r^2 + r'^2 + 2rr'\cos\varphi')^{1/2}$. ϕ_{eff} is the effective quantum yield, which is proportional to the photosensitizers concentration.

If absorptions are added to this white medium both for the excitation and emission light, the corresponding fluorescence intensities can be derived from $F(\mu_{s0}^x, \mu_{s0}^m, \mu_a^x = 0, \mu_a^m = 0, r, t_1, t_2)$ with the Beer-Lambert law:

$$F(\mu_s^x, \mu_s^m, \mu_a^x, \mu_a^m, r, t_1, t_2) = F(\mu_s^x, \mu_s^m, \mu_a^x = 0, \mu_a^m = 0, r, t_1, t_2) \exp(-\mu_a^x v t_1) \exp(-\mu_a^m v t_2) \qquad (2)$$

where $v = c/n$. Integrate over the time delay t_1 and t_2, and the distance r, we will get

$$\iiint_{t_1,t_2,r} \mathrm{d}t_1 \mathrm{d}t_2 \mathrm{d}r F(\mu_s^x, \mu_s^m, \mu_a^x, \mu_a^m, r, t_1, t_2) = \iiint_{t_1,t_2,r} \mathrm{d}t_1 \mathrm{d}t_2 \mathrm{d}r F(\mu_s^x, \mu_s^m, \mu_a^x = 0, \mu_a^m = 0, r, t_1, t_2) \exp(-\mu_a^x v t_1 - \mu_a^m v t_2) =$$

$$\equiv \left(\iiint_{t_1,t_2,r} \mathrm{d}t_1 \mathrm{d}t_2 \mathrm{d}r F(\mu_s^x, \mu_s^m, \mu_a^x = 0, \mu_a^m = 0, r, t_1, t_2) \right) \exp(-\Delta) \qquad (3)$$

By further defining a correction factor for compensating the attenuation due to the tissue absorption both for the excitation and emission

$$\exp(\Delta) = \frac{\iiint_{t_1,t_2,r} \mathrm{d}t_1 \mathrm{d}t_2 \mathrm{d}r F(\mu_s^x, \mu_s^m, \mu_a^x = 0, \mu_a^m = 0, r, t_1, t_2)}{\iiint_{t_1,t_2,r} \mathrm{d}t_1 \mathrm{d}t_2 \mathrm{d}r F(\mu_s^x, \mu_s^m, \mu_a^x = 0, \mu_a^m = 0, r, t_1, t_2) \exp(-\mu_a^x v t_1 - \mu_a^m v t_2)} \qquad (4)$$

It is note worthy to point out that the term $\iiint_{t_1,t_2,r} \mathrm{d}t_1 \mathrm{d}t_2 \mathrm{d}r F(\mu_s^x, \mu_s^m, \mu_a^x, \mu_a^m, r, t_1, t_2)$ in Eq. 2 corresponds to the measured fluorescence intensity, F_{meas}. Then take Eq. 1 into account, we have

$$F_{meas} \exp(\Delta) \propto \iiint_{t_1,t_2,r} \mathrm{d}t_1 \mathrm{d}t_2 \mathrm{d}r F(\mu_s^x, \mu_s^m, \mu_a^x = 0, \mu_a^m = 0, r, t_1, t_2) \propto \phi_{eff} \propto \text{sensitizer concentration} \qquad (5)$$

3. Results and discussion

The tissue was assumed to be homogeneous and the sensitizer to be uniformly distributed. All images from the animal measurements were prior to processing cropped to the size of the organs. The fluorescence intensity for an image was computed as the average over the total organ. Fig. 1 shows the correlation between the raw fluorescence signals and the sensitizer concentrations for the murine livers and kidneys. The poor correlations obviously show that turbid tissue does play an important role in the measured fluorescence. Meanwhile tissue autofluorescence, the profile of the laser beam, tissue inhomogeneity, and so forth also contribute.

To compensate the attenuation caused by tissue, the optical properties for different organs need to be known. The values from literatures vary much and are not consistent with each organ sample. Therefore we firstly tested our method with tissue-like phantoms. The concentrations of Rhodamine 6G and absorption coefficients of the phantoms (here $\mu_a^m = \mu_a^m = \mu_a$) are given in Fig. 2. The scattering coefficients are $\mu_s^x = 77.42\ \mathrm{cm}^{-1}$ and $\mu_s^m = 63.85\ \mathrm{cm}^{-1}$, respectively. The anisotropic factor $g^x = g^m = 0.87$. Fig. 2 shows the correlation between the fluorescence in a logarithm scale and dye concentrations before and after the attenuation correction. The crosses

BTuD6.pdf

illustrate that the fluorescence from the surface is heavily dependent on the optical properties. The intrinsic fluorescence (circles) from the fluorophores, achieved by multiplying the measured intensities with a simulated correction factor (as defined in Eq. 4), has an extremely good correlation to the dye concentrations.

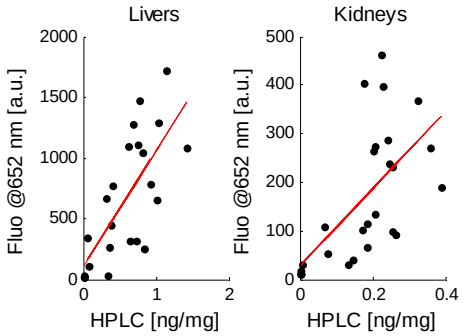

Fig. 1. Scatter plot and a linear fit of the data, showing the correlation between the raw fluorescence intensities and HPLC values.

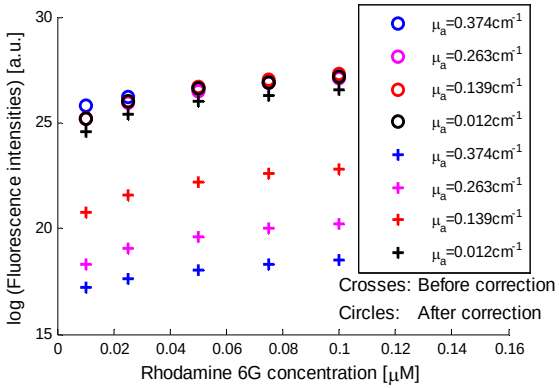

Fig.2. Correlations between the fluorescence intensities and dye concentrations for liquid tissue phantoms.

For the animal case, Fig.3 shows that the simulated correction factor, which can compensate for the tissue attenuation both for the excitation and emission, depends much more on tissue absorption than scattering coefficients. The approach gives a correction factor for different organs investigated, yielding an intrinsic fluorescence intensity and thus accurate concentration of the drug. Results from different organs and drug to light intervals will be presented.

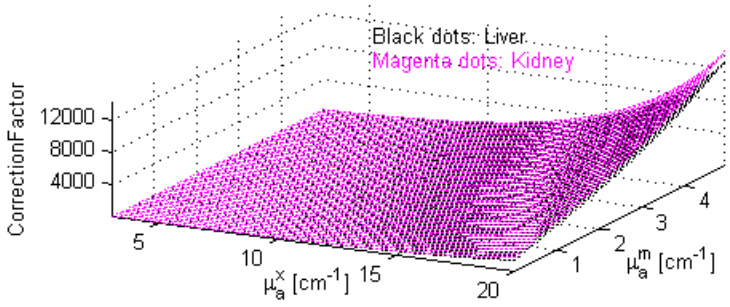

Fig.3 Dependence of the correction factor on tissue absorption coefficients for murine tissue, where $\mu_s^x = 57.5\text{cm}^{-1}$, $\mu_s^m = 35\text{cm}^{-1}$, g = 0.8 for liver, and $\mu_s^x = 240\text{cm}^{-1}$, $\mu_s^m = 117\text{cm}^{-1}$, g = 0.8 for kidney [4] were used.

4. Conclusion

In conclusion, a new approach combining fluorescence imaging and FWMC simulation is presented to accurately study the intrinsic fluorescence information and photosensizer concentration distribution in murine tissue. This approach offers a great advantage of minimizing the dependence on the tissue optical properties. It can be applied to *in vivo* drug quantification, surgical guidance, tumor delineation, and so forth.

Acknowledgements

We gratefully acknowledge financial support from the EU Brighter project, and the Linneus grant to LLC.

References

[1] G. Themelis, J. Yoo, K. Soh, R. Schulz, and V. Ntziachristos, "Real-time intraoperative fluorescence imaging system using light-absorption correction," J. Biomed. Opt. Vol. **14**, 064012 (2009).

[2] E. Alerstam, S. Andersson-Engels, and T. Svensson, "White Monte Carlo for time-resolved photon migration," J. Biomed. Opt. **13**, 041304 (2008).

[3] J. Swartling, A. Pifferi, A. M. K. Enejder, and S. Andersson-Engels, "Accelerated Monte Carlo models to simulate fluorescence spectra from layered tissues," J. Opt. Soc. Am. *A* **20**(4), 714–727 (2003).

[4] G.Alexandrakis, F.Rannou, and A. Chatziioannou, "Tomographic bioluminescence imaging by use of a combined optical-PET (OPET) system: a computer simulation feasibility study," Phys. Med. Biol. **50** 4225-4241 (2005).